Sasikumar, A., Trias, D., Costa, J., Singery, V. i Linde, P. (2019). Mitigating the weak impact response of thin-ply based thin laminates through an unsymmetrical laminate design incorporating intermediate grade plies. *Composite Structures*, vol. 220, p. 93-104. Available online at
https://doi.org/10.1016/j.compstruct.2019.03.069

Mitigating the weak impact response of thin-ply based thin laminates through an unsymmetrical laminate design incorporating intermediate grade plies

A.Sasikumar[a,*], D.Trias[a,1], J. Costa[a,*], V. Singery[b], P.Linde[c,d]

[a] *AMADE, Polytechnic School, University of Girona, Campus Montilivi s/n, 17073 Girona, Spain*
[b] *Chomarat, 39 Avenue de Chabannes, 07160 Le Cheylard, France*
[c] *Airbus Operations GmbH, Kreetslag 10, 21129 Hamburg, Germany*
[d] *Department of Industrial and Materials Science, Chalmers University of Technology, S-41296 Gothenburg, Sweden*

Abstract

With aeronautic industries focussing on thinner structures and reducing manufacturing costs, recent research has been dedicated to the impact and post impact response of thin laminates (< 2 mm) made of textile fabric composites. A recent study revealed that thin laminates based on thin plies exhibit extensive fibre failure and reduced compression after impact strength. To mitigate this weakness, we propose a novel laminate concept based on combining plies of different thicknesses in an unsymmetrical configuration (intermediate grade plies are located only at the bottom of the laminate, i.e., the non-impacted face). C-scan inspection on impacted and quasi-statically indented specimens, allowed the damage sequence of the proposed unsymmetrical hybrid laminate to be compared with that of the thin-ply baseline. The hybrid laminate with intermediate plies at the bottom, delayed and reduced the fibre damage, decreased the projected delamination area and led to a 30% increase in the compression after impact strength in contrast to the thin-ply baseline laminate.

Keywords:
Hybrid laminates, Non-crimp fabrics, Impact behaviour, Damage tolerance, Unsymmetrical laminates

1. Introduction

In the quest to reduce structural weight, aircraft manufacturers are considering using thin structures, especially for the fuselage and wing skins. One of the main difficulties with these thin structures (< 2 mm) is their increased vulnerability to out-of-plane loads, coupled with a high reduction in the residual strength during the post-impact service cycles of the aircraft [1]. Recent research has reported that a low velocity impact (enough to create a barely visible impact damage on the laminate) has caused a 60-70% reduction in the compressive strength of thin laminates [2; 3]. This alarming reduction has led aircraft manufacturers to consider non-conventional laminate designs, not only as

☆

*Corresponding author : Aravind Sasikumar, Josep Costa
Email addresses: aravind.sasikumar@udg.edu (A.Sasikumar), josep.costa@udg.edu (J. Costa)

[1] Serra Húnter Fellow

an economic way to reduce the severity of impact damage but also to improve the compression after impact (CAI) strength.

Despite the vast amount of impact studies performed on thick laminates [4–9] (4-5 mm, as suggested in the ASTM standard [10]), very few studies have been dedicated towards thin laminates and their response to impact and CAI loads. Recently, Garcia et al. [11] discussed the effect ply thickness has on the out-of-plane response of 2.15 mm laminates made of non-crimp fabrics using tomographic investigations. The current authors [3] compared the effect fabric architecture and ply thickness have on impact and CAI strength of thin laminates (1.6 - 1.8 mm), where two types of fabrics, namely woven and non-crimp fabrics, were studied. Results revealed that, unlike thick laminates [5; 12], thin laminates made of thin plies resulted in extensive fibre damage which led to reduced CAI strength. Meanwhile, intermediate ply grades, even though they exhibited early damage onset in terms of delamination, had comparably lesser fibre damage, and led to greater CAI strength than thin plies had [3; 11].

Concerning non-conventional laminate designs, in a recent work [2], the authors proposed mixing uni-directional (UD) plies of different thickness grades to produce hybrid thin laminates. One of the hybrid designs (where thick 0° plies were added close to the laminate mid-plane symmetry along with thin plies) demonstrated a significant improvement in CAI strength (40%) when compared to the thin-ply baseline laminate. This study promised that by using a hybrid laminate the potential benefits of the different ply grades can be exploited through ply level hybridization, as is also demonstrated in [13–15]. Despite the novelty of hybridization, the laminate mid-plane symmetry constraint found in the studies and which restricts the laminate to having the same top sub-laminate layup mirrored below the symmetry plane, was still adhered. Because damage from an impact induces unsymmetrical damage modes in the laminate thickness direction, it is necessary to move away from the conventional symmetry designs and also to enlarge the stacking sequence design space. In a preliminary study with thick laminates and using plies of same thicknesses [16], the authors demonstrated that the mid-plane symmetry can be challenged without the worry of warping and from this the laminate can be tailored towards impact loads by having different top and bottom sub-laminates.

These two concepts (unsymmetry and ply hybridization) could be combined into a laminate design where thick plies can be mixed with thin plies to form a hybrid laminate. At the same time, the thicker plies can be placed at a desired location without having to worry about placing equivalent thick plies on the other side of the laminate's mid-plane symmetry line. By employing this design idea, an attempt is made to tailor the damage in an impact scenario which, will in turn, could help to improve the CAI strength. According to the authors' knowledge, this is the first work reporting on the impact and CAI response of such novel laminate designs. In this paper, we designed a hybrid and unsymmetrical laminate (with zero warp) using non-crimp fabrics where intermediate plies had been added to thin plies to form a hybrid laminate. Within the framework of thin laminates (1.6 mm), we carried out an experimental study to investigate the impact and CAI response of this novel laminate design. In addition, we also compared the results with those of the baseline laminates (symmetric and non-hybrid), where one laminate was made only of intermediate plies and the other with only thin plies (baseline results presented by the authors in [3]). We also performed quasi-static indentation tests interrupted for C-scan inspection, to compare the damage initiation and evolution between the hybrid and the baseline laminates. Experimental results reveal that the proposed novel laminate design could tailor the impact damage with less fibre breakage and thereby considerably improve the CAI strength over the thin-ply baseline laminate.

2. Laminate design

2.1. Material

We used bi-axial non-crimp fabrics (NCF), where two differently oriented fibre tows are stitched together using a polyester yarn. The double axis layup of the NCF blankets reduces the manufacturing costs significantly [17]. The material system used is a carbon fibre T700 pre-impregnated with HexPly® M21 resin. Bi-axial prepreg blankets of [0°/45°] and [0°/-45°] which can also lead to other orientations through flipping and/or rotation, were used. We employed two different fabric thickness grades: 268 and 134 gsm, so the UD ply thickness corresponds to 0.134 and 0.067 mm, and, in this paper, referred to as intermediate and thin ply grade, respectively.

2.2. Rationale behind the laminate design

From the experimental results reported in [2; 3], the thin laminates, unlike the thick laminates, underwent considerable bending under impact loads and the high in-plane tensile loads led to fibre splitting at the back face of the laminate. The thin laminates made of thin plies, delayed delamination but exhibited extensive back fibre splitting, while the intermediate ply grades displayed an early delamination onset, but with a reduced fibre damage. Hence, to exploit the potential of both ply grades (i.e., the ability of intermediate plies to reduce fibre damage by dissipating energy through delaminations and thin plies to delay damage onset, along with higher plain compression strength they possess [3]), we propose a hybrid laminate design, where intermediate plies are added to a thin-ply NCF laminate.

Furthermore, it is equally important to decide in which through-the-thickness location in the laminate, the intermediate plies have to be added. As the non-impacted face of the laminate is prone to extensive fibre splitting when used with thin plies, our intention was to add intermediate plies at the non-impacted laminate face, in an attempt to reduce fibre breakage by promoting delamination. Hence, this demands an unsymmetrical laminate design with a minimum bending stretching coupling matrix ([B]) to avoid warpage during manufacturing [18].

2.3. Unsymmetrical hybrid laminate design: Optimization

We used an optimization algorithm (a genetic algorithm embedded in the MATLAB optimization toolbox [19]) to search for unsymmetrical laminate designs with a minimum or null B value. The objective function was to minimize the sum of B matrix terms, and the constraints were as given below:

- Balanced and quasi-isotropic laminate.
- Four plies (two NCF blankets) of intermediate ply grade as bottom plies (at the non-impacted face of the laminate)
- As the outer plies are affected by impactor indentation (impacted face) and fibre splitting (non-impacted face), they were fixed to be 90° as they are comparatively the least influential on the CAI strength. For the same reason, the 0° plies were restricted from being placed in the outer NCF blankets.
- The equivalent bending stiffness parameter (D*, proposed by Olsson [20] and applied as an optimization constraint in [21]) is made to match within 1% of the value of the baseline laminates to have a proper comparison.

A solution (an unsymmetrical-hybrid laminate with null B matrix) satisfying all the constraints was obtained and is provided along with details in the following section.

2.4. Laminates and stacking sequences

The unsymmetrical-hybrid laminate (with zero B matrix) obtained is provided in Table 1, and hereafter will be referred to as NCF-UHB, denoting 'Unsymmetrical Hybrid laminate with intermediate plies at Bottom' (non-impacted side). The same laminate is flipped upside down to have an 'Unsymmetrical Hybrid laminate with the intermediate plies at the Top' (impacted side), and will be referred to as NCF-UHT. The objective of introducing the NCF-UHT laminate is to understand the effect the location (at impacted or non-impacted side) of the added intermediate plies has on the impact and CAI response. To study the effect of hybridization, the two unsymmetrical hybrid laminates are compared to baseline laminates, namely NCF-Int and NCF-Thin (results published by the authors in a recent work [3]). NCF-Int and NCF-Thin are symmetrical laminates made using only one ply grade, namely intermediate and thin ply grades, respectively. It is also important to recall that NCF-UHB and NCF-UHT are thin-ply dominant (comprising of 67% thin plies and 33% intermediate grade plies for the laminate thickness) hybrid laminates. All four laminates and their stacking sequences are illustrated in Fig. 1 and Table 1 provides further laminate details.

Figs. 2 (a) and (b) present the polar plots of the in-plane and bending stiffnesses, respectively, of all the laminates. Note that the baseline laminates are in-plane non-quasi isotropic, while the proposed unsymmetrical laminates are in-plane quasi-isotropic. The maximum deviation of the equivalent bending stiffnesses (D*) between the proposed and the baseline laminates is less than 0.2%, hence the difference is negligible in terms of the practical application of these laminates.

[Table 1 about here.]

[Figure 1 about here.]

[Figure 2 about here.]

3. Experimental methods

Impact specimens of dimensions 150 x 100 mm were cut from the panels with 0° plies aligned with the specimen length. NCF-UHB specimens were flipped upside down to obtain NCF-UHT specimens, i.e., the one with the intermediate plies at the top. Note that flipping a laminate upside down only interchanges the 45° plies by -45° and vice-versa. We performed the impact tests in accordance with the ASTM D7136/D7136-15 standard [22], using a CEAST Fractovis Plus instrumented drop-weight tower. A 16 mm steel hemispherical indenter was used and the total mass of the impactor setup was set to 3 kg.

Three impact energies, 6.4 J, 8.2 J and 10.5 J, (the same energies as used in [3] for the baseline laminates NCF-Int and NCF-Thin) were explored, and hereafter will be referred to as IE_1, IE_2 and IE_3, respectively. We impacted nine specimens per laminate, with three specimens for each impact energy, to assess the repeatability. Further details of the experimental impact setup can be found in [23].

We performed quasi-static indentation (QSI) tests with an MTS INSIGHT® 50 testing machine with a 50 kN load cell and displacement controlled loading of the indenter. 150 x 100 mm specimens were placed on a base plate, which has an open window of 125 x 75 mm. Four rubber clamps were used to fasten the specimen to the base plate. A constant indenter displacement of 1 mm/min was used. We explored a total of seven indenter displacements, the same as in [3], for comparison purposes. A total of three specimens per laminate were used for the QSI tests, where a same specimen was loaded and then interrupted for C-scan damage inspection and then followed by a higher indenter displacement loading. The damage was inspected after impact and after each QSI loading level using a pulse-echo ultrasonic C-scan technique. The C-scan setup featured an OLYMPUS OMNI MX system along with a 5 MHz piezoelectric probe.

To evaluate the post-impact compressive strength, CAI tests were performed on the impacted specimens using an MTS INSIGHT®300 machine with a 300 kN load cell, following the ASTM D7317/D7137M-15 [10]. To account for the reduced laminate thickness, we used an additional anti-buckling device (proposed by Remacha et al. [24]) along with the CAI fixture. The additional fixture ensured the specimen was refrained from global buckling, thus ensuring a proper compressive failure at the specimen's impacted site. Furthermore, to evaluate the pristine compression strength, plain compression strength tests were performed in accordance with the ASTM D6484/D6484M-14 standard [25]. Three 305 x 30 mm specimens were tested with a cross head displacement of 1 mm/min for the plain compression strength at the INEGI research facility at the University of Porto. All the above tests, except plain compression strength, were performed at the AMADE research laboratory (NADCAP certified for non-metallic material testing) at the University of Girona.

4. Results

4.1. Impact

Figs. 3, 4 and 5 present the impact force-time, impact force-deflection and impact energy-time curves, respectively, of all four laminates. Note that, due to good repeatability, only one specimen data per laminate per energy level is presented. Inspecting the curves in Figs. 3 and 4, a clear difference in the impact response is seen between NCF-UHB and NCF-UHT, indicating the effect the location of the added intermediate plies has on the impact response.

For the lowest energy level IE_1, no load drop was observed with NCF-UHB, which also exhibited the maximum peak force (3200 N) compared to all other laminates. To the contrary, NCF-UHT exhibited its first significant load drop close to 2200 N, followed by further load drops, thereby leading to a suppressed load carrying capability compared to NCF-UHB. Moving on to the higher energies (IE_2 and IE_3), NCF-UHB displayed first significant load drop close to the peak load (3500 N) followed by successive drops. In reviewing the impact curves in Figs. 3 and 4, the laminates can be grouped in terms of their similar responses, for instance, NCF-Int and NCF-UHB in one group, and NCF-Thin and NCF-UHT in the other. Similar behaviour was observed with the energy evolution curves (Fig. 5) where NCF-UHB dissipated significantly less energy than NCF-UHT for all impact energies explored. While NCF-UHB had the least dissipated energy for IE_1, at higher energies it dissipated more energy than NCF-Int, but still significantly less than NCF-Thin and NCF-UHT.

[Figure 3 about here.]

[Figure 4 about here.]

[Figure 5 about here.]

Fig. 6 compares the projected impact damage profile for the four laminates obtained from C-scan inspection. The projected damage area, the dominant delaminations and their corresponding interfaces are also marked in the same figure. The thin-ply laminate NCF-Thin exhibited the highest projected damage area while the hybrid NCF-UHB displayed the least. It is important to note that both the hybrid laminates considerably reduced the damage area compared to their baselines. While NCF-Int had dominant delaminations at interface 10 (bottom interface) and 6 (interface just below the mid-plane) oriented at 45° and 22.5°, respectively, NCF-Thin exhibited a dominant delamination at interface 12 (just below the mid-plane ply cluster), as reported in [3].

With the hybrid designs, NCF-UHB displayed a dominant delamination at the last interface (int. 18 (-45°/90°), at the site of the intermediate grade plies added at the laminate bottom) oriented at 90°, as predicted during the laminate design phase. At the highest impact energy, the total projected damage area is governed by this single last interface delamination, where the other delaminations are found to be comparatively negligible (see Fig. 6). For NCF-UHT, interfaces 5 (0°/45°) and 10 (45°/90°) exhibited dominant delaminations, with orientations at 45° and 90°, respectively. Contrary to NCF-UHB, many interfaces contributed towards the total projected damage area of NCF-UHT. While NCF-UHB had dominant delamination at the non-impacted site where the intermediate plies were added, NCF-UHT exhibited dominant delaminations just below the added intermediate plies (at and just below the mid-plane).

[Figure 6 about here.]

Fig. 7 presents the photos of the impacted and non-impacted faces of all the laminates from the 10.5 J impact. The impact dent depth at the impacted face and the fibre splitting (in the orientation of the last ply) at the non-impacted face can be visually compared between the four laminates. While the thin ply NCF-Thin exhibited the highest magnitude of impact dent depth and extensive fibre splitting, the intermediate-ply laminate NCF-Int comparatively suppressed both these parameters, as reported in [3]. The hybrid laminates, despite being a thin-ply dominant laminate, exhibited reduced back fibre splitting compared to its baseline NCF-Thin due to the inclusion of the intermediate plies.

[Figure 7 about here.]

Figs. 8(a) and (b) represent the evolution of the peak load and projected damage area, respectively, for increasing impact energies, while Figs. 9 (a) and (b) present the dissipated energy and impact dent depth against the impact energies, respectively. Out of all the laminates, NCF-Thin possessed the least load carrying capability, as evidenced by the least peak load (Fig. 8(a)). NCF-UHB and NCF-Int displayed similar values, despite NCF-UHB having slightly higher values for the first two energies. Compared to the baseline NCF-Thin, NCF-UHB exhibited a 30% higher peak force considering all the impact energies. In terms of the projected damage area, both hybrid laminates exhibited less area compared to the baselines, whereas NCF-Thin displayed the greatest damage area. NCF-UHB laminate showed the smallest damage area, with a significant reduction of 50% and 20% over the thin ply baseline NCF-Thin and the intermediate ply baseline NCF-Int, respectively (Fig. 8(b)).

[Figure 8 about here.]

[Figure 9 about here.]

NCF-Int and NCF-UHB exhibited the least dissipated energy, while NCF-Thin and NCF-UHT dissipated the highest. NCF-UHB exhibited a 30% reduction in the dissipated energy over NCF-Thin. We observed similar responses with the impact dent depth, where the thin-ply laminate NCF-Thin exhibited the highest dent depth followed by the hybrid laminate NCF-UHT. NCF-Int and NCF-UHB suppressed the impact dent depth compared to the other two laminates, where NCF-UHB displayed a 50% reduced dent depth compared to the thin ply baseline NCF-Thin.

4.2. Quasi-static indentation

Fig. 10 compares the force-deflection responses of the two hybrid laminates along with that of the baselines for the highest indenter deflection of d_7= 6 mm. Other indenter deflections studied (d_1 to d_6) are also marked on the same figure. As already reported in [3], NCF-Int exhibited the first load drop at around 3500 N, close to the maximum peak load. To the contrary, NCF-Thin exhibited an early load drop, at around 2000 N, followed by successive load drops leading to a reduced maximum load (as also observed in the impact results). With the hybrid laminates, NCF-UHT behaved similar to NCF-Thin, with early and intermittent load drops, whereas NCF-UHB displayed a similar response to that of NCF-Int with the first load drop occurring at the peak load. Compared to thin-ply baseline NCF-Thin, interestingly, both hybrid laminates delayed the first load drop. NCF-UHB and NCF-UHT, respectively, exhibited a 55% (3300 N) and 15% (2400 N) increase in the force value at which the first load drop was observed (attributed to fibre damage initiation), when compared to NCF-Thin.

Fig. 11 presents the C-scan images of the damage profile for all the indenter displacement levels for all the laminates. The figure also presents the applied energy and projected damage area for each displacement, identified delaminated interfaces and the initiation of fibre splitting (marked by 'FS' denoting fibre split in Fig. 11), observed by visual inspection of the non-impacted surface. It is evident that intermediate plies (NCF-Int) displayed early delamination at d_1, even though no associated load drop was seen in the force-deflection response. There was no sign of damage in the other three laminates at d_1. At d_2, NCF-UHB showed the first instance of delamination, identified at the last interface (int 18: (-45°/90°)). NCF-Thin and NCF-UHT delayed the onset of damage, the first instance of which was observed at d_3, whereas damage had already been propagated in NCF-Int and

NCF-UHB. Delamination onset was identified in NCF-UHT at the top sub-laminate (just below the added intermediate plies) at interface 5 (0°/45°). Moving on to d_4, NCF-Thin exhibited back fibre splitting associated with the load drop (see Fig. 10) between d_3 and d_4. On further loading, the dominant delamination was identifed in NCF-UHB at the last interface (at the bottom, within the added intermediate plies) and at the mid-plane (int 7: (90°/-45°)) for NCF-UHT. With continued loading, NCF-UHT displayed fibre splits associated with the load drop between d_5 and d_6. The highest indenter displacement d_7 marked the onset of fibre splits on NCF-Int and NCF-UHB, also indicated by the high load drops seen in their respective curves. It is interesting to note that both hybrid laminates exhibited 50% reduced damage area compared to the thin-ply baseline NCF-Thin. The QSI results (mainly the force-deflection curves, the damage profile and the first load drop) are coherent with the impact results. While the initiation of delamination is hidden in the force response curves of these thin laminates [3], the load drops correspond to the initiation and extension of fibre damage.

[Figure 10 about here.]

[Figure 11 about here.]

Fig. 12 presents the evolution of the dissipated energies (E_d) against the applied energies (E_a) for the different QSI deflection levels. The applied energies are calculated by integrating the area under the whole loading part of the respective QSI curves, while the dissipated energy is the area of the enclosed curve obtained. Until the applied energy of 4 J, NCF-Thin dissipated the least energy while for energies higher than 4 J, the same laminate dissipated the highest energy. At higher applied energies (above E_a of 5 J), both NCF-UHB and NCF-Int exhibited lower dissipated energies compared to NCF-Thin and NCF-UHT. NCF-UHB dissipated 50% and 60% less energy, respectively, when compared to its counterparts NCF-UHT and NCF-Thin.

[Figure 12 about here.]

4.3. Compression after impact

Fig. 13 presents the pristine compression and CAI strength of all the laminates for all the impact energies. With intermediate and thin plies mixed in the same laminate, the hybrid laminate exhibited a plain compression strength value in between that of NCF-Int and NCF-Thin. NCF-UHT and NCF-UHB displayed a 5% lower plain compression strength than the thin-ply laminate and a 5% higher value than NCF-Int. As reported in [2; 3], thin plies have a higher pristine compression strength (10% increase) over the intermediate plies. Note that the thin-ply laminate NCF-Thin at IE_1 exhibited invalid CAI failure mode (caused by local buckling at the top of the specimen as reported in [3]) despite using the anti-buckling ribs.

[Figure 13 about here.]

Out of all the laminates and all the energies, the hybrid laminate NCF-UHB exhibited the highest CAI strength. Figs. 14 (a) and (b) present the plain compression and CAI strengths of the hybrid laminates normalized with respect to the baselines NCF-Int and NCF-Thin, respectively. On comparing NCF-UHB laminate to the baselines when reviewing all the impact energies, NCF-UHB exhibited 12% and 30% higher CAI strength over NCF-Int and NCF-Thin, respectively. Between the two hybrid laminates, NCF-UHB displayed 20% more CAI strength than NCF-UHT, indicating the importance the location of the added intermediate plies has on the post-impact response. NCF-UHT exhibited higher CAI strength that the baselines for IE_1, but at higher impact energies (IE_2 and IE_3) the CAI strength dropped drastically and exhibited similar values to those of NCF-Thin. Fig. 15 shows the reduction in the residual compression strength caused by the impact damage for all laminates. NCF-Thin displayed the highest reduction (60%) in the compression strength, while NCF-UHB showed the lowest (40%).

[Figure 14 about here.]

[Figure 15 about here.]

5. Discussion

Thin laminates undergo severe bending during impact loading due to their reduced bending stiffness [2; 3]. Bending induces high in-plane tensile stresses at the non-impacted face of the laminate that leads to fibre splits or breakage in the bottom plies (Fig. 7). In addition, high bending creates shear stresses between the plies that trigger delamination at the interfaces closest to the bottom of the laminate. Studies on thin laminates [2; 26] reveal that the bottom interfaces (close to the non-impacted face) exhibit extensive delamination. Hence, the non-impacted face is the most critical or damage prone region in a thin laminate under low velocity impact loads, as evidenced by the delamination and fibre damage at this location.

As reported in [3], irrespective of the ply grade of non-crimp fabrics used, low velocity impact loads induce both delamination and fibre damage in thin laminates. However, the extent of the dominance of these damage modes depends significantly on the ply grade used. Thin laminates made of thin plies exhibited delayed delamination onset (associated to their in-situ effect [27; 28]), but with early and extended fibre damage. To the contrary, thicker plies dissipated energy through matrix cracks and delaminations, resulting in delayed and subdued fibre damage. Increased fibre damage with thin plies resulted in poor impact response (reduced peak loads and high energy dissipation) and a reduced CAI strength (as in NCF-Thin).

Unlike thin plies, intermediate plies (or a cluster of two thin plies) introduce higher interlaminar shear stresses at their adjacent interfaces (resulting from the high bending stiffness mismatch between the interfaces [29]) triggering delamination [23]. C-scan images of NCF-UHB revealed the dominant delamination at the last laminate interface, within the site of the added intermediate plies, thereby following the hypothesis formulated during the laminate design phase. On the other hand, impact loading induces high out-of-plane compressive stresses at the impactor vicinity and these stresses counteract the interlaminar shear stresses to increase the local interlaminar fracture toughness [30]. This explains the absence of dominant delaminations within the region of the added intermediate plies (at the top) in NCF-UHT.

The addition of the intermediate plies to the bottom of the laminate (critical region) resulted in suppressing/delaying the fibre damage by promoting early delamination. This is evidenced in the QSI results by the 55% increase in the force value over NCF-Thin at which the first load drop was observed (associated with the initiation of fibre damage). Meanwhile, the addition of intermediate plies to the top of the laminate helped to delay the initiation of fibre damage compared to NCF-Thin (as in Fig. 10) but with the critical bottom part of the laminate comprised of thin plies, fibre damage was dominant (evidenced by the successive load drops in Figs. 4 and 10).

CAI strength of a thin laminate depends on the extent of delamination and fibre damage in the laminate, with fibre damage being more critical and clearly linked to the drastic reduction in the CAI strength [2; 31]. On one hand, the already formed delaminations split the laminate into sub-laminates, and one of the sub-laminates buckles to result in a final collapse. On the other hand, a high magnitude of fibre failure in the laminate, especially the load sustaining 0° plies, promotes compressive fibre failure that leads to CAI failure. In NCF-UHB, the C-scan inspection reveals that entire damage area is significantly lower than that of the baselines and also governed by a single delamination at the last interface, oriented in the 90° direction. Hence, under CAI loads, the laminate will split with a thicker sub-laminate at the top (entire laminate except the last ply) and a thinner one at the bottom (last ply, 90°) which is not carrying a high load. The thicker sub-laminate sustains higher compressive loads leading to a higher CAI strength [32]. In addition to this, the reduced fibre failure, as a result of hybridization, is also a reason for the increased CAI strength. Meanwhile, the increased fibre damage in NCF-UHT laminate led to its reduced CAI strength, compared to its flipped counterpart.

While thin plies have been a remarkable asset to the composite community with their numerous advantages (delamination resistance [33], associated in-situ strength), their vulnerability towards impact and post impact loads is their Achilles heel. In this study, we have exhibited that the addition of some thicker plies could substantially mitigate the out-of-plane threats to a thin-ply laminate, evidenced in the form of reduced fibre failure, delamination area and higher CAI strength. The results show that hybridization can be used to exploit the potential of different ply grades and help in tailoring the damage to occur at predetermined locations. Apart from the unsymmetrical design helping to understand the importance the location of added plies has, they can be the optimal solution for several load cases. When compared to the expensive alternatives of modifying the material system or using interface toughening agents to improve the out-of-plane response of thin plies, we have demonstrated the full potential laminate design has to come up with novel laminates promising remarkable improvements, and also economic feasibility. While in this study we proposed the idea of a novel laminate as a rule of thumb, the next immediate step is to explore all the laminates within a particular design space to find an optimum damage-tolerant laminate using numerical finite element tools.

6. Conclusion

Impact loads pose a great threat to thin laminates made of thin plies because of the extensive fibre failure and reduced CAI strength. To alleviate this vulnerability thin plies have towards out-of-plane responses, we have made a first attempt to design a novel laminate which combines ply hybridization and laminate mid-plane unsymmetry. We designed a hybrid laminate (made of non-crimp fabrics) which comprises both thin and intermediate plies, where the intermediate plies are placed only on the non-impacted side of the laminate (NCF-UHB). We carried out an experimental campaign using impact, compression after impact and quasi-static indentation tests and compared the responses of the proposed laminate to those of the symmetric and non-hybrid baseline laminates. We also included in the comparison the hybrid laminate flipped upside down (NCF-UHT, intermediate plies at the top) to illustrate how crucial is the location of the intermediate plies. The hybrid laminate NCF-UHB substantially delayed the fibre breakage onset (by 55%) and reduced the extent of fibre damage when compared to the thin-ply baseline NCF-Thin. The proposed laminate exhibited a 50% and 30% reduction in damage area and dissipated energy, respectively, over the thin-ply baseline laminate, thus providing a higher impact resistance. As a result of the improved impact response, the unsymmetrical-hybrid laminate increased the CAI strength by 30% (over the thin-ply baseline). In view of a practical application of the proposed novel design, for the baseline laminate to match the same residual strength as of the proposed laminate, additional plies have to be added to the baseline laminate, which in turn results in added mass and increased material costs. Finally, we have demonstrated the prospects of this novel laminate design (combining hybridization and unsymmetry) as an efficient and economic tool to mitigate the weakness of thin plies towards impact and post impact loads.

Acknowledgements

The first author would like to thank the Generalitat de Catalunya for the FI-DGR pre-doctoral grant (2018 FI-B2 00118). The authors would like to thank Chomarat at Le Cheylard, France, for providing the materials used in this study. This work has been supported by the *Spanish Ministerio de Economía y Competitividad* through the grant coded MAT2015-69491-C3-1-R, supported by FEDER/EU. The baseline laminates for comparison purposes are from a research project led by Airbus, partnered with AMADE (University of Girona, Spain), INEGI (University of Porto, Portugal), and the University of Dayton Research Institute (UDRI, US). Thanks to Airborne Composites at Girona, Spain, for manufacturing the unsymmetrical laminates.

Data Availability

The raw/processed data required to reproduce these findings cannot be shared at this time due to legal or ethical reasons.

References

[1] S. Abrate, Impact on Composite Structures, Cambridge University Press, 2005.

[2] A. Sasikumar, D. Trias, J. Costa, J. Orr, P. Linde, Effect of ply thickness and ply hybridization on compression after impact strength of thin composite laminates, Submitted to Composites Part A: Applied Science and Manufacturing.

[3] A. Sasikumar, D. Trias, J. Costa, N. Blanco, J. Orr, P. Linde, Impact and compression after impact response in thin laminates of spread-tow woven and non-crimp fabrics, Composite Structures 215 (2019) 432–445.

[4] H. Saito, M. Morita, K. Kawabe, M. Kanesaki, H. Takeuchi, M. Tanaka, I. Kimpara, Effect of ply-thickness on impact damage morphology in CFRP laminates, Journal of Reinforced Plastics and Composites 30 (13) (2011) 1097–1106.

[5] T. Yokozeki, Y. Aoki, T. Ogasawara, Experimental characterization of strength and damage resistance properties of thin-ply carbon fiber/toughened epoxy laminates, Composite Structures 82 (3) (2008) 382–389.

[6] M. U. Saeed, Z. Chen, Z. Chen, B. Li, Compression behavior of laminated composites subjected to damage induced by low velocity impact and drilling, Composites Part B: Engineering 56 (2014) 815–820.

[7] S. Sihn, R. Y. Kim, K. Kawabe, S. W. Tsai, Experimental studies of thin-ply laminated composites, Composites Science and Technology 67 (6) (2007) 996–1008.

[8] Y. Liv, G. Guillamet, J. Costa, E. González, L. Marín, J. Mayugo, Experimental study into compression after impact strength of laminates with conventional and nonconventional ply orientations, Composites Part B: Engineering 126 (2017) 133–142.

[9] F. Caputo, A. De Luca, R. Sepe, Numerical study of the structural behaviour of impacted composite laminates subjected to compression load, Composites Part B: Engineering 79 (2015) 456–465.

[10] ASTM D7137/D7137-15, Standard Test Method for Compressive Residual Strength Properties of Damaged Polymer Matrix Composite Plates, 2015.

[11] S. García-Rodríguez, J. Costa, A. Bardera, V. Singery, D. Trias, A 3D tomographic investigation to elucidate the low-velocity impact resistance, tolerance and damage sequence of thin non-crimp fabric laminates: effect of ply-thickness, Composites Part A: Applied Science and Manufacturing 113 (2018) 53–65.

[12] J. Cugnoni, R. Amacher, S. Kohler, J. Brunner, E. Kramer, C. Dransfeld, W. Smith, K. Scobbie, L. Sorensen, J. Botsis, Towards aerospace grade thin-ply composites: Effect of ply thickness, fibre, matrix and interlayer toughening on strength and damage tolerance, Composites Science and Technology 168 (2018) 467–477.

[13] T. Sebaey, E. Mahdi, Using thin-plies to improve the damage resistance and tolerance of aeronautical CFRP composites, Composites Part A: Applied Science and Manufacturing 86 (2016) 31–38.

[14] A. Arteiro, G. Catalanotti, J. Xavier, P. Linde, P. Camanho, A strategy to improve the structural performance of non-crimp fabric thin-ply laminates, Composite Structures 188 (2018) 438–449.

[15] C. Furtado, A. Arteiro, G. Catalanotti, J. Xavier, P. Camanho, Selective ply-level hybridisation for improved notched response of composite laminates, Composite Structures 145 (2016) 1–14.

[16] A. Sasikumar, J. Costa, D. Trias, E. V. González, S. García-Rodríguez, P. Maimí, Unsymmetrical stacking sequences as a novel approach to tailor damage resistance under out-of-plane impact loading,, Composites Science and Technology 173 (2019) 125–135.

[17] S. W. Tsai, M. Cognet, The amazing bi-angle thin-ply NCF, JEC composites (68) (2011) 51–52.

[18] C. T. Herakovich, Mechanics of fibrous composites, 1998.

[19] MATLAB, version 8.5.0 (R2015a), The MathWorks Inc., Natick, Massachusetts, 2015.

[20] R. Olsson, Closed form prediction of peak load and delamination onset under small mass impact, Composite Structures 59 (3) (2003) 341–349.

[21] T. Sebaey, E. González, C. Lopes, N. Blanco, P. Maimí, J. Costa, Damage resistance and damage tolerance of dispersed CFRP laminates: Effect of the mismatch angle between plies, Composite Structures 101 (2013) 255–264.

[22] ASTM D7136/D7136-15, Standard test method for measuring the damage resistance of a fiber reinforced polymer matrix composite to a drop weight impact event, 2015.

[23] E. González, P. Maimí, P. Camanho, C. Lopes, N. Blanco, Effects of ply clustering in laminated composite plates under low-velocity impact loading, Composites Science and Technology 71 (6) (2011) 805–817.

[24] M. Remacha, S. Sánchez-Sáez, B. López-Romano, E. Barbero, A new device for determining the compression after impact strength in thin laminates, Composite Structures 127 (2015) 99–107.

[25] ASTM D6484/D6484M-09, Standard test method for open-hole compressive strength of polymer matrix composite laminates, 2009.

[26] S. García-Rodríguez, J. Costa, V. Singery, I. Boada, J. Mayugo, The effect interleaving has on thin-ply non-crimp fabric laminate impact response: X-ray tomography investigation, Composites Part A: Applied Science and Manufacturing 107 (2018) 409–420.

[27] P. P. Camanho, C. G. Dávila, S. T. Pinho, L. Iannucci, P. Robinson, Prediction of in situ strengths and matrix cracking in composites under transverse tension and in-plane shear, Composites Part A: Applied Science and Manufacturing 37 (2) (2006) 165–176.

[28] P. P. Camanho, P. Maimí, C. Dávila, Prediction of size effects in notched laminates using continuum damage mechanics, Composites Science and Technology 67 (13) (2007) 2715–2727.

[29] D. Liu, Impact-induced delamination—a view of bending stiffness mismatching, Journal of Composite Materials 22 (7) (1988) 674–692.

[30] G. Catalanotti, C. Furtado, T. Scalici, G. Pitarresi, F. Van Der Meer, P. Camanho, The effect of through-thickness compressive stress on mode II interlaminar fracture toughness, Composite Structures 182 (2017) 153–163.

[31] D. Ghelli, G. Minak, Low velocity impact and compression after impact tests on thin carbon/epoxy laminates, Composites Part B: Engineering 42 (7) (2011) 2067–2079.

[32] S.-F. Hwang, G.-H. Liu, Buckling behavior of composite laminates with multiple delaminations under uniaxial compression, Composite structures 53 (2) (2001) 235–243.

[33] G. Guillamet, A. Turon, J. Costa, J. Renart, P. Linde, J. Mayugo, Damage occurrence at edges of non-crimp-fabric thin-ply laminates under off-axis uniaxial loading, Composites Science and Technology 98 (2014) 44–50.

List of Figures

List of Tables

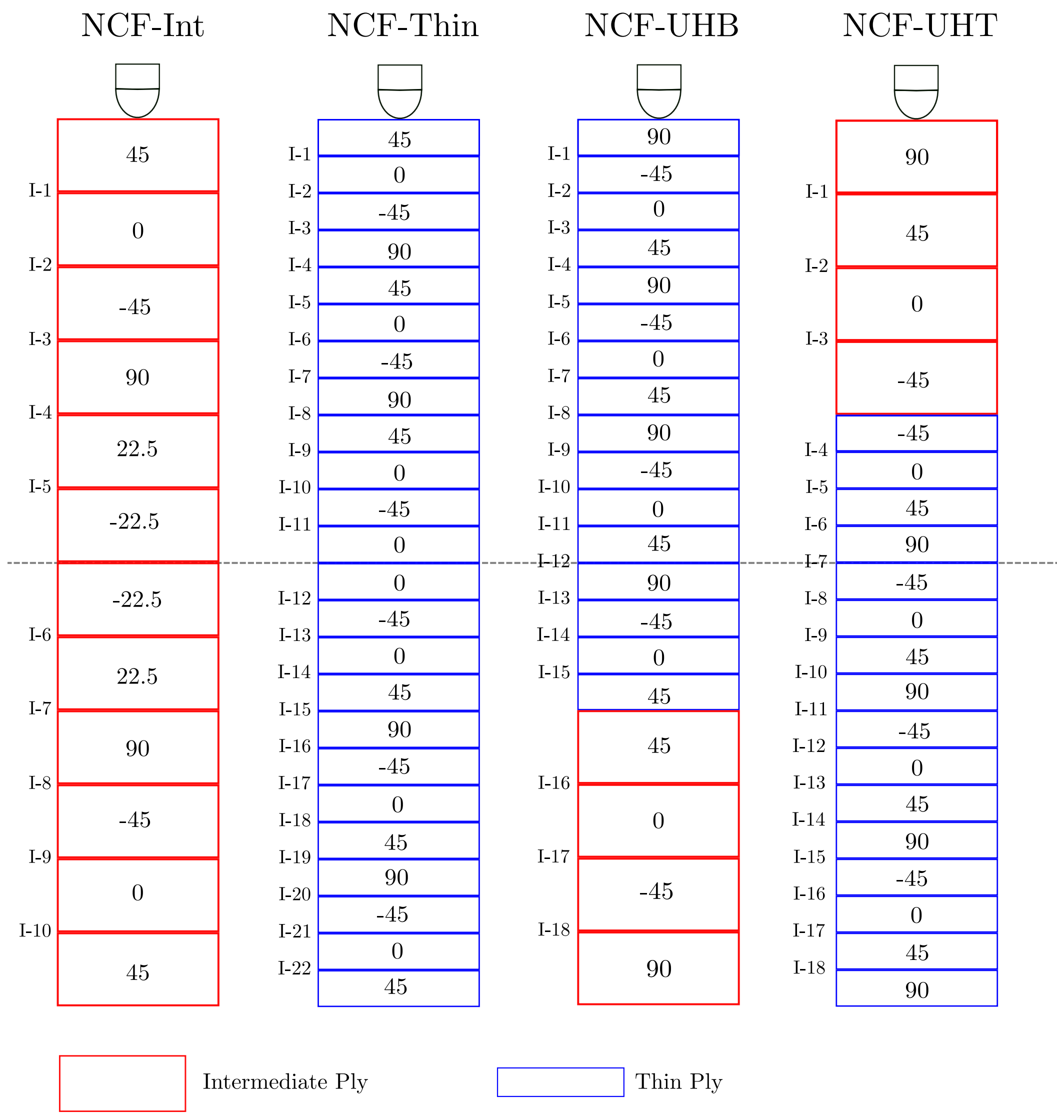

Figure 1: Illustration of all the laminates used for the study: NCF-Int, NCF-Thin, NCF-UHB and NCF-UHT, where NCF-UHT is obtained by flipping NCF-UHB upside down. Note that U refers to unsymmetry, H to hybrid design, T and B to top and bottom (location of intermediate grade plies).

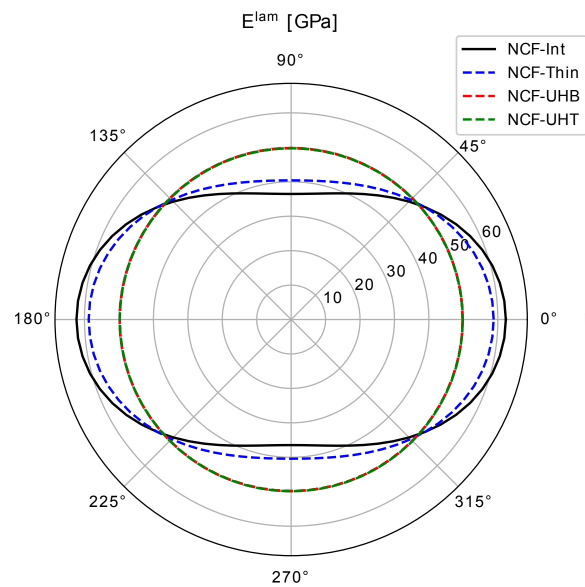

(a)

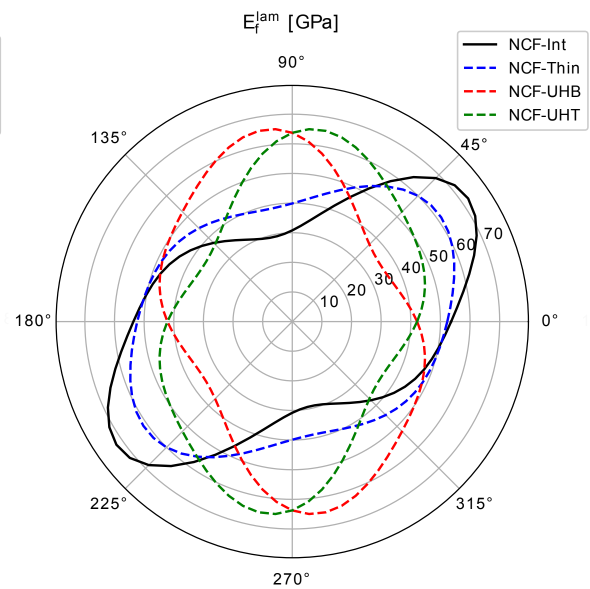

(b)

Figure 2: Polar plot representation of the (a) in-plane stiffness and (b) bending stiffness of all the laminates.

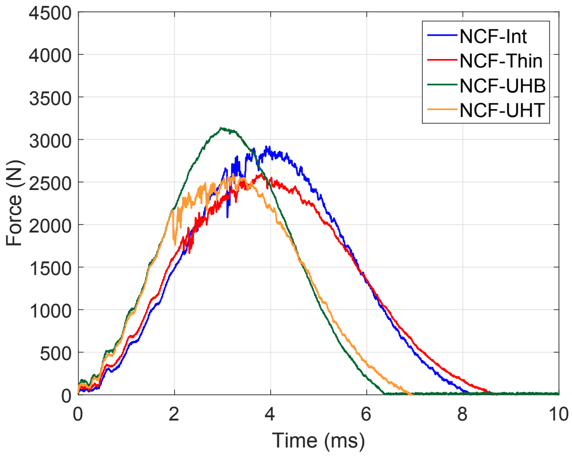

(a) IE_1

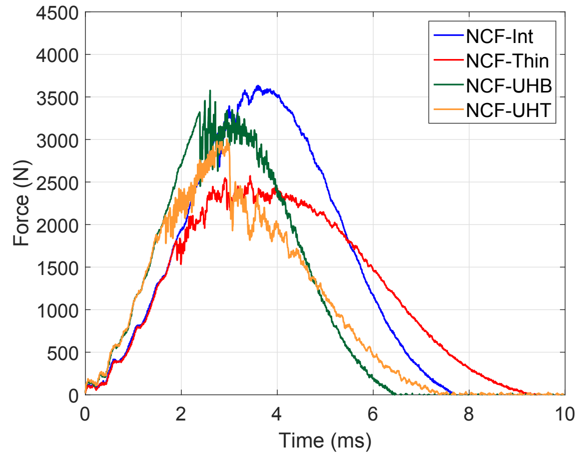

(b) IE_2

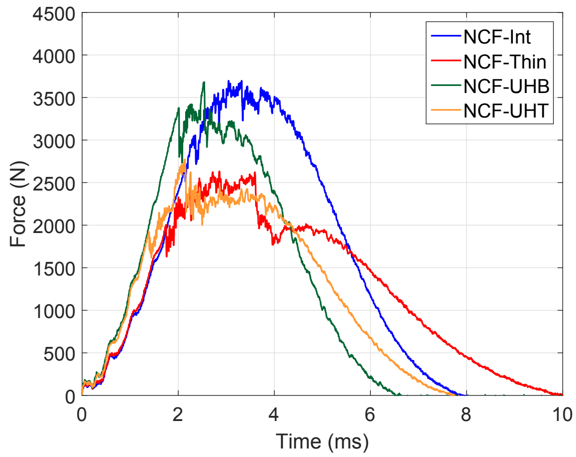

(c) IE_3

Figure 3: Impact force-time response curves of all laminates for all three impact energies.

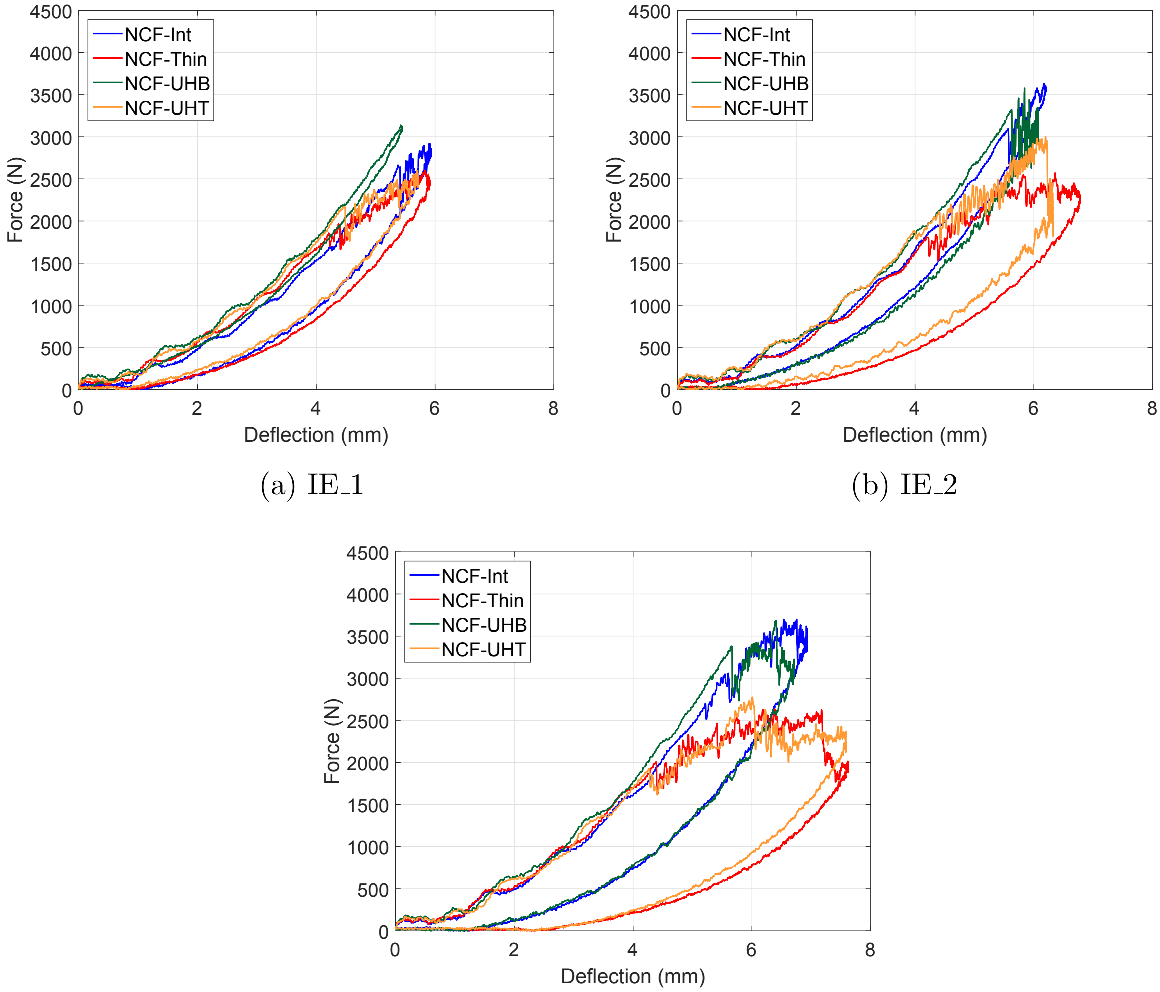

(a) IE_1

(b) IE_2

(c) IE_3

Figure 4: Impact force-deflection response curves of all laminates for all three impact energies.

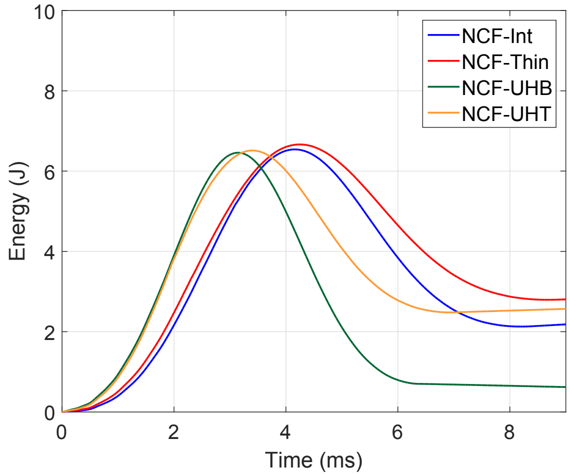

(a) IE_1

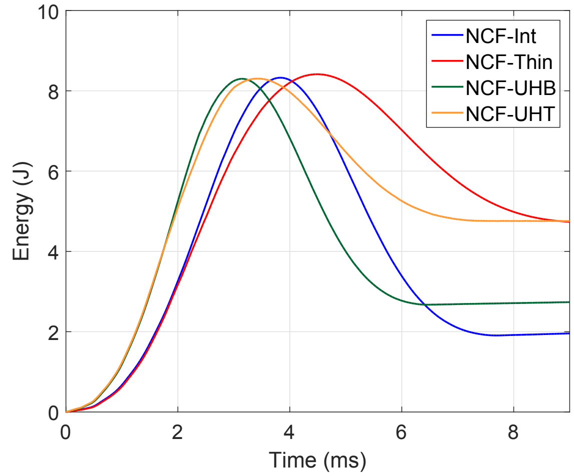

(b) IE_2

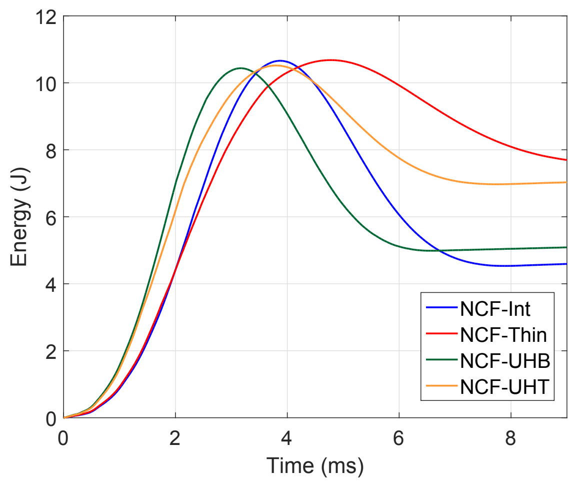

(c) IE_3

Figure 5: Impact energy evolution curves of all laminates for all three impact energies.

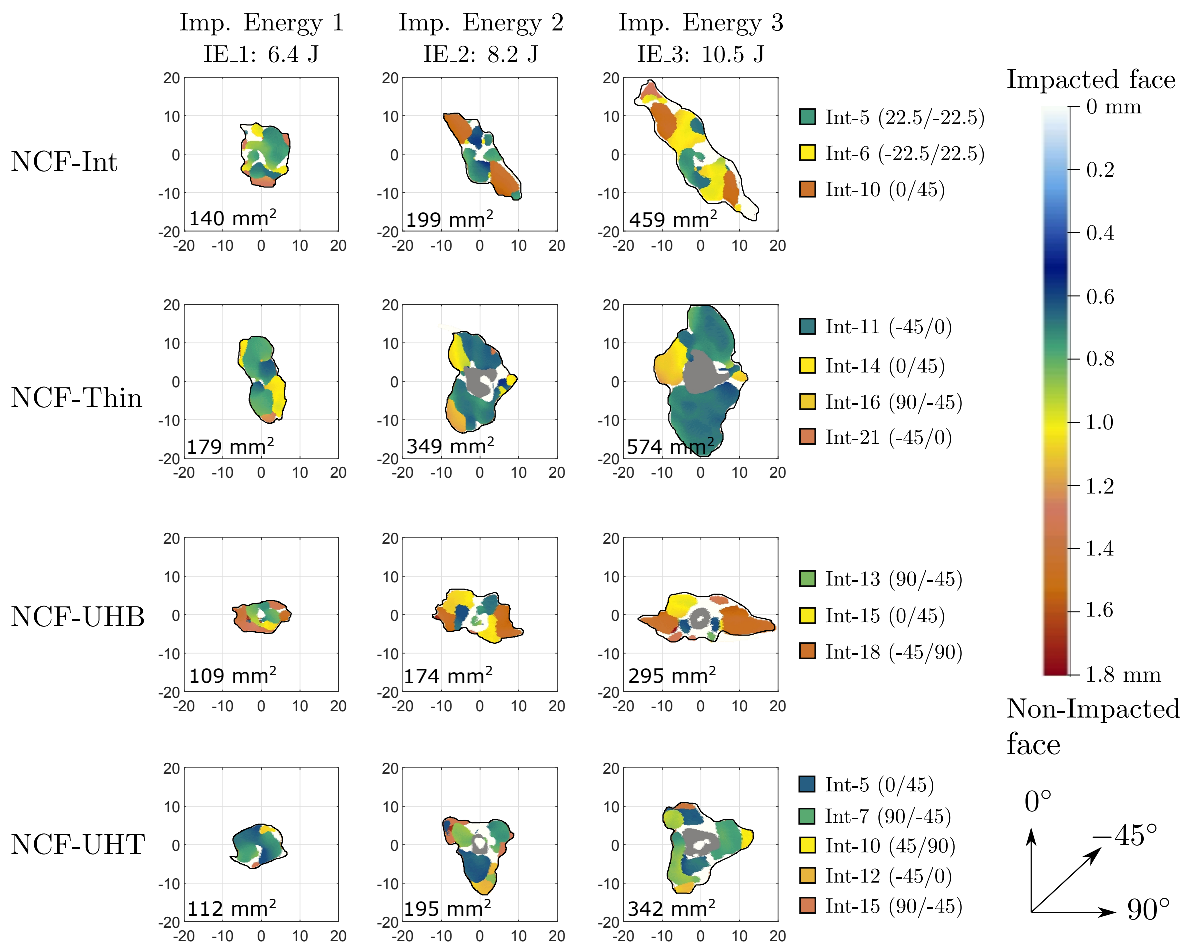

Figure 6: C-scan inspection images of all laminates along with the projected damage areas and the dominant delaminations identified (the field of inspection presented is a 40 x 40 mm square window with impacted site as the centre).

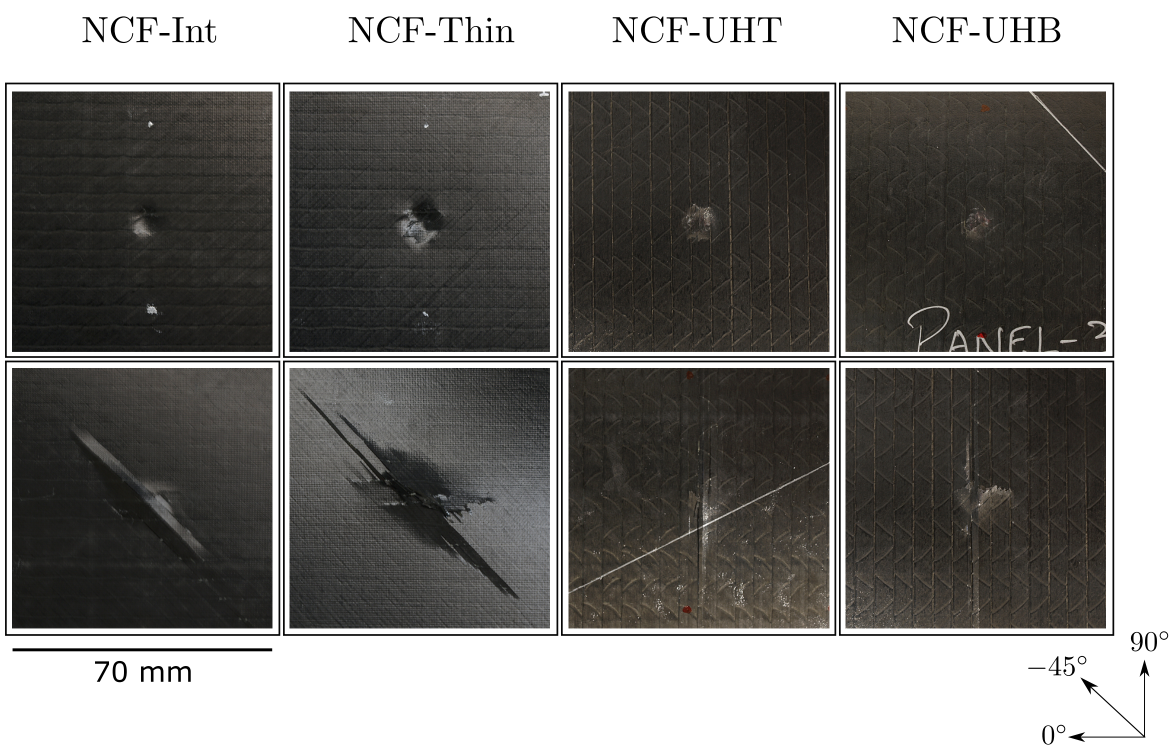

Figure 7: Impact (top) and non-impacted (bottom) laminate face photos of all laminates after the 10.5 J impact (represented field of view is a 70 x 70 mm square window with the impacted site as the centre).

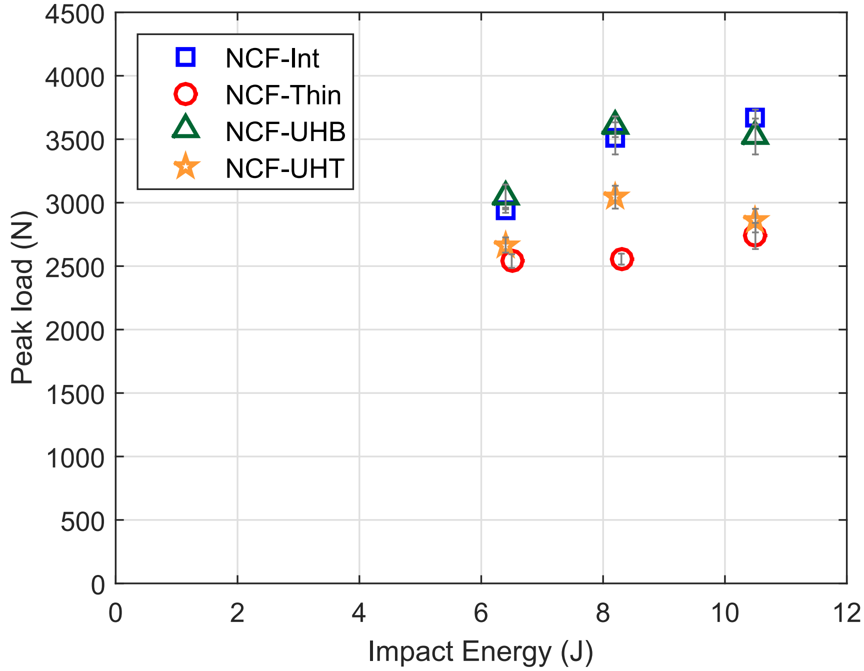

(a)

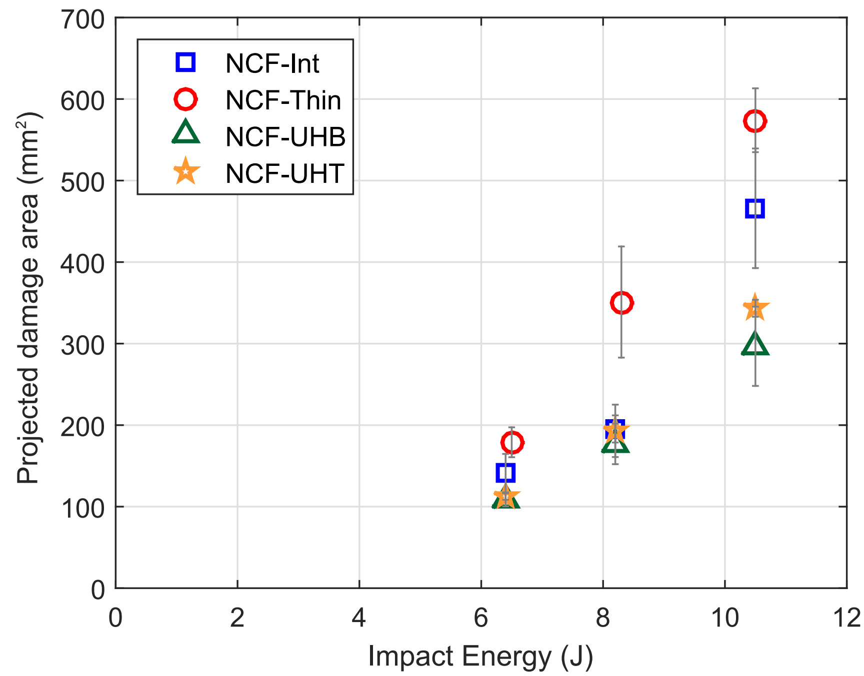

(b)

Figure 8: Impact damage resistance parameters (a) peak load and (b) projected damage area compared between all the laminates for all the impact energies (average value is presented along with the standard deviation indicated by the vertical markers).

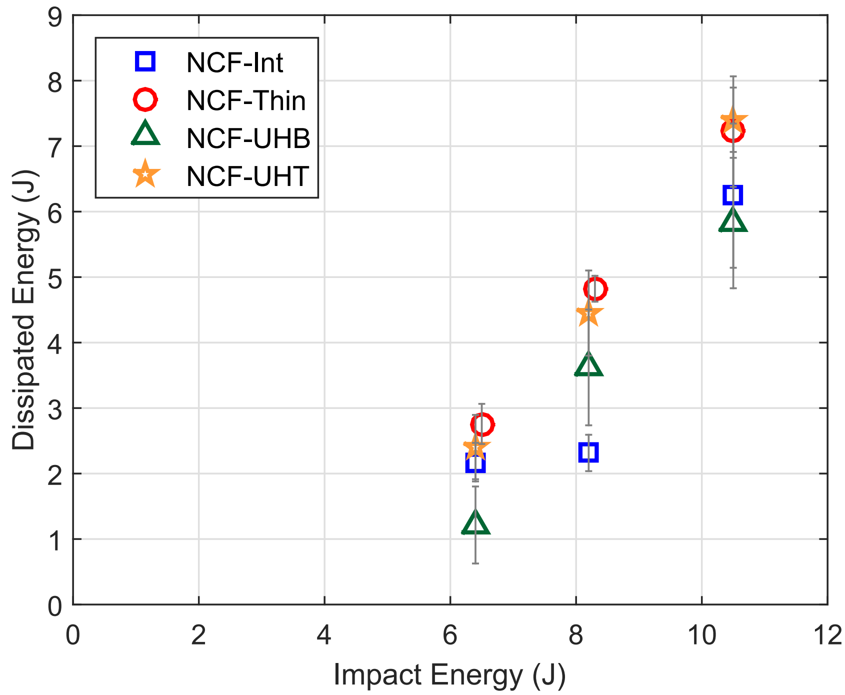

(a)

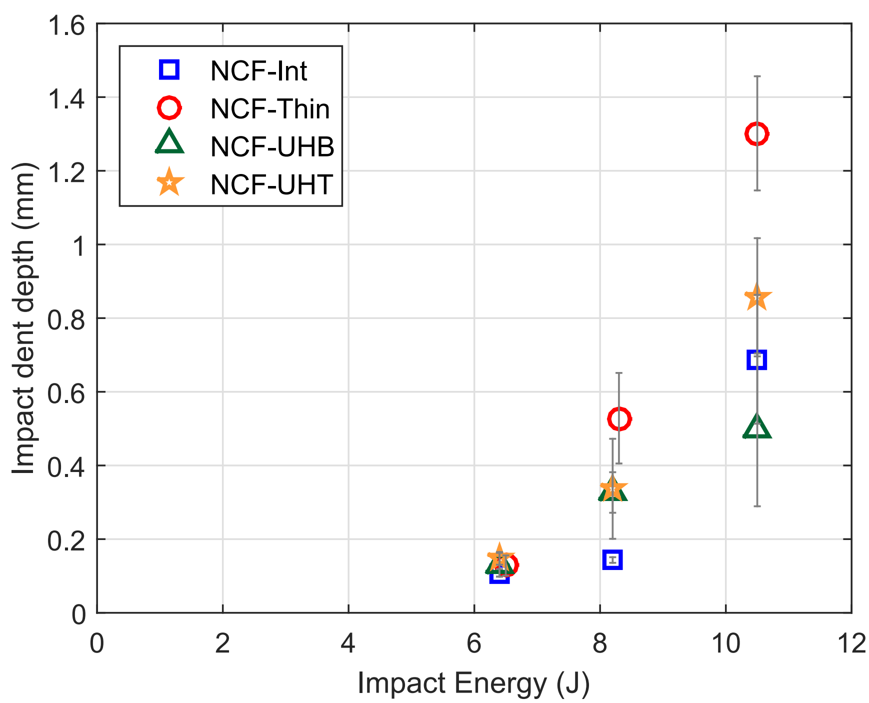

(b)

Figure 9: Impact damage resistance parameters (a) dissipated energy and (b) impact dent depth compared between all the laminates for all absolute impact energies (average value is presented along with the standard deviation indicated by the vertical markers).

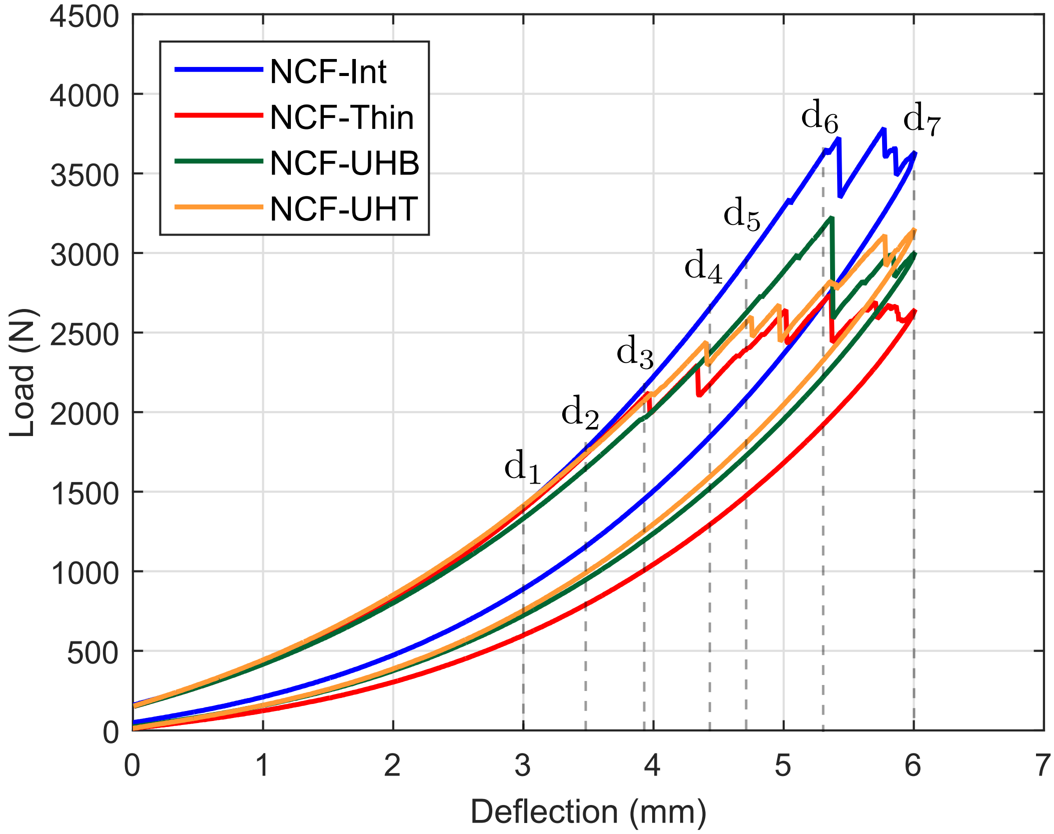

Figure 10: QSI load deflection responses of all laminates for the highest deflection d_7=6 mm, and the other indenter deflections studied (d_1 to d_6) are also marked.

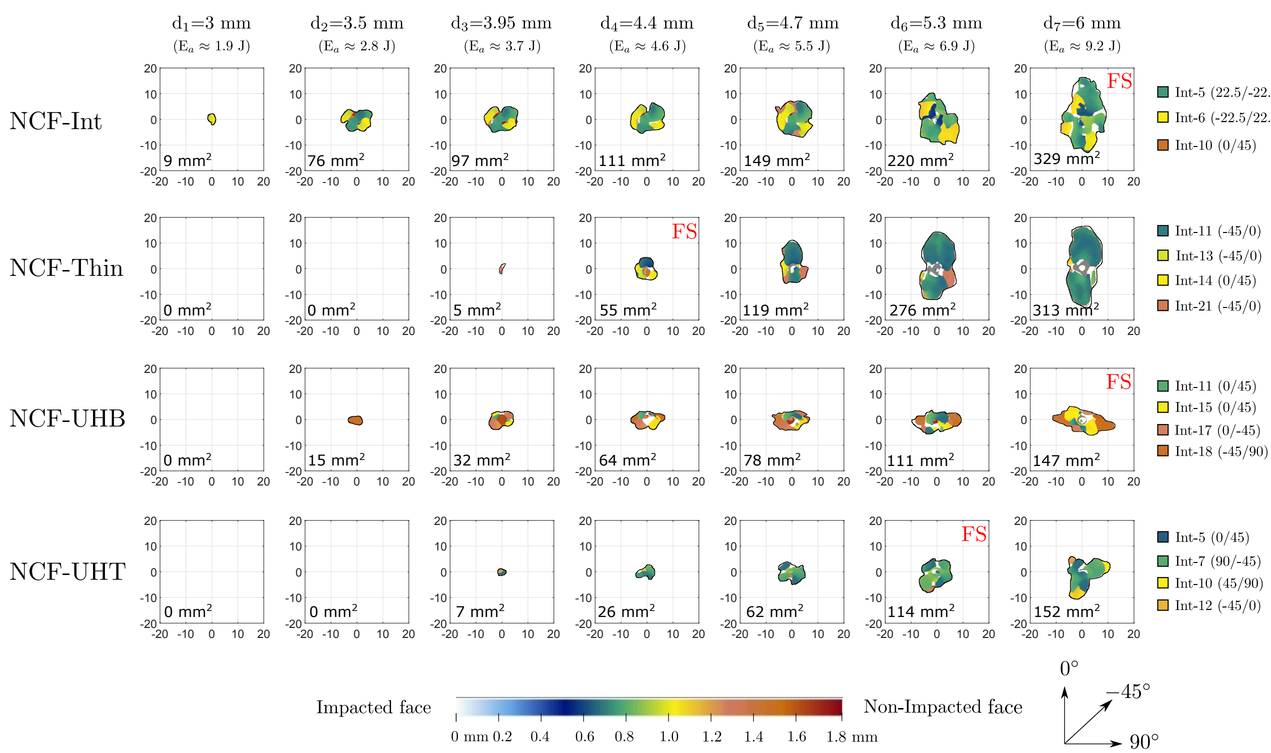

Figure 11: C-scan inspection images for all laminates for all the indenter deflections from d_1 to d_7. Projected damage profile and area are presented, furthermore the initiation of back fibre splitting is also identified and marked by 'FS'.

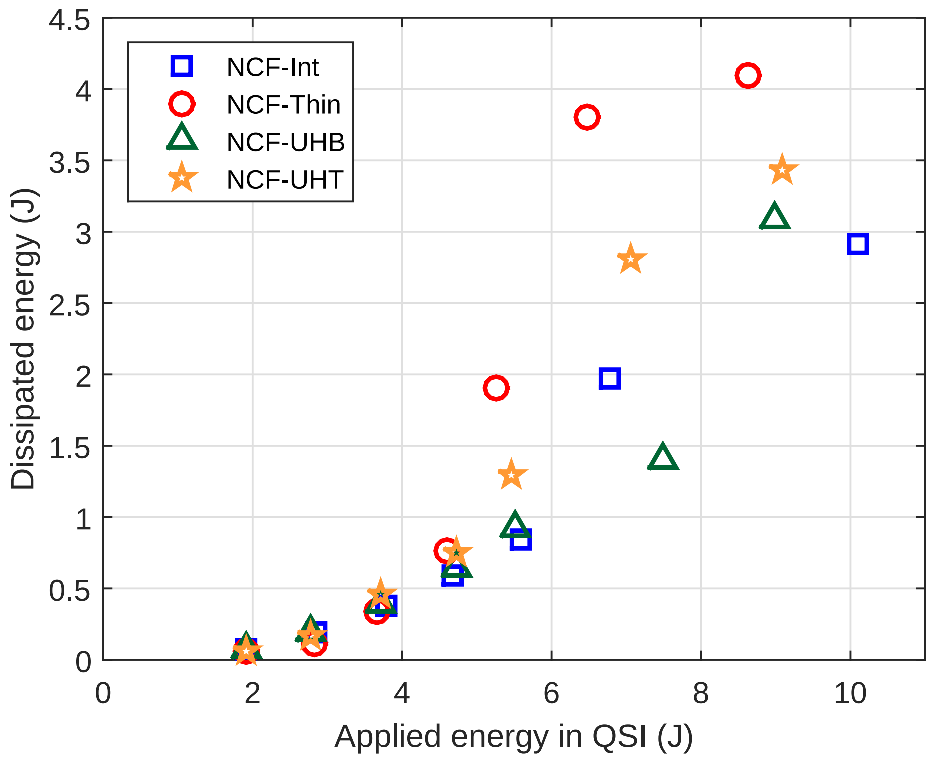

Figure 12: The evolution of dissipated energy (E_d) plotted against the applied energies (E_a) for all seven QSI deflection levels for all laminates

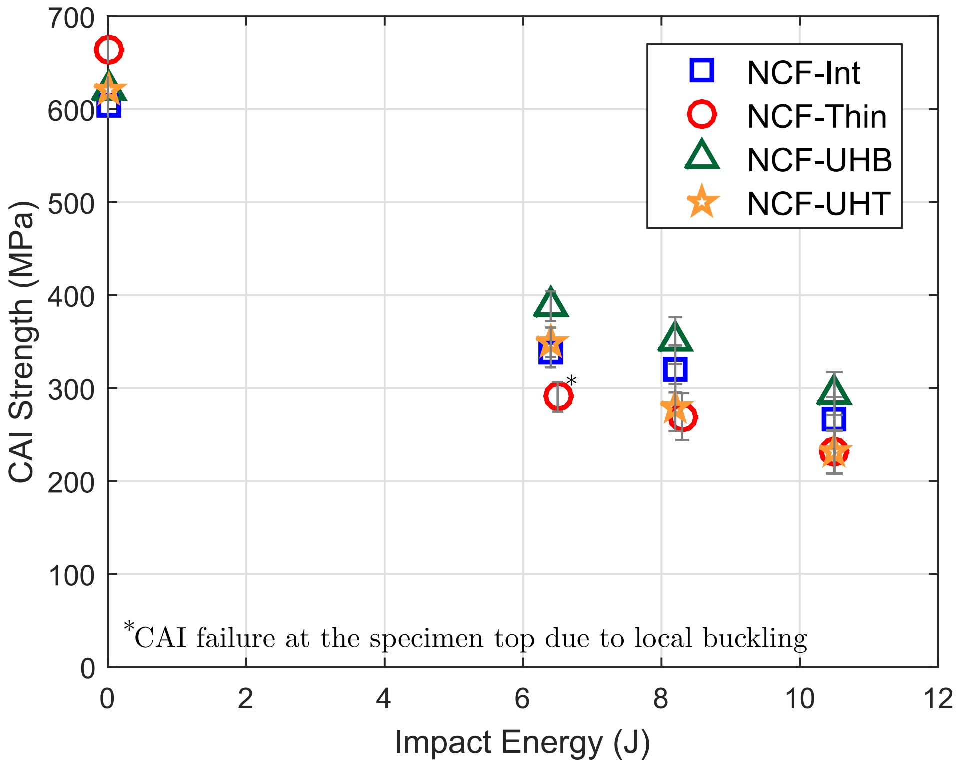

Figure 13: Plain compression strengths and CAI strengths of all laminates for all impact energies

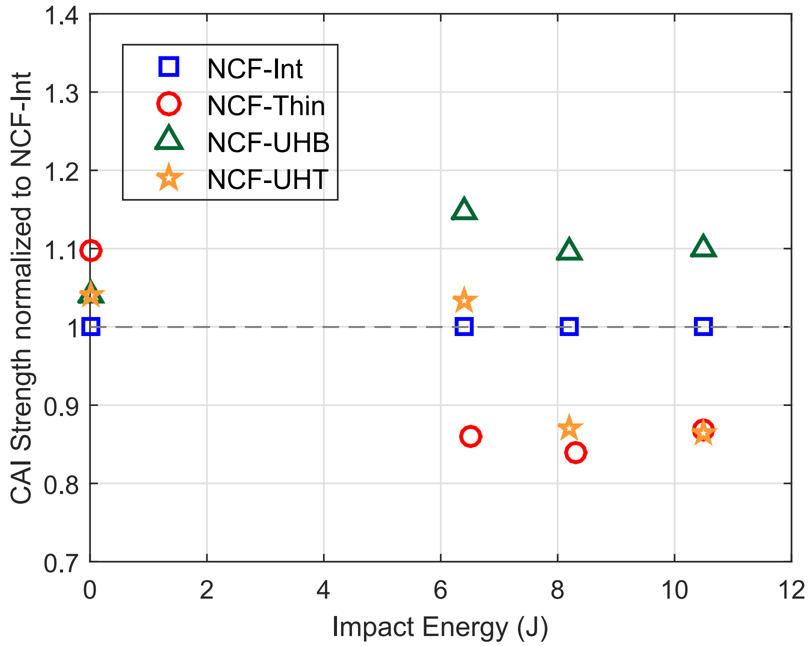

(a)

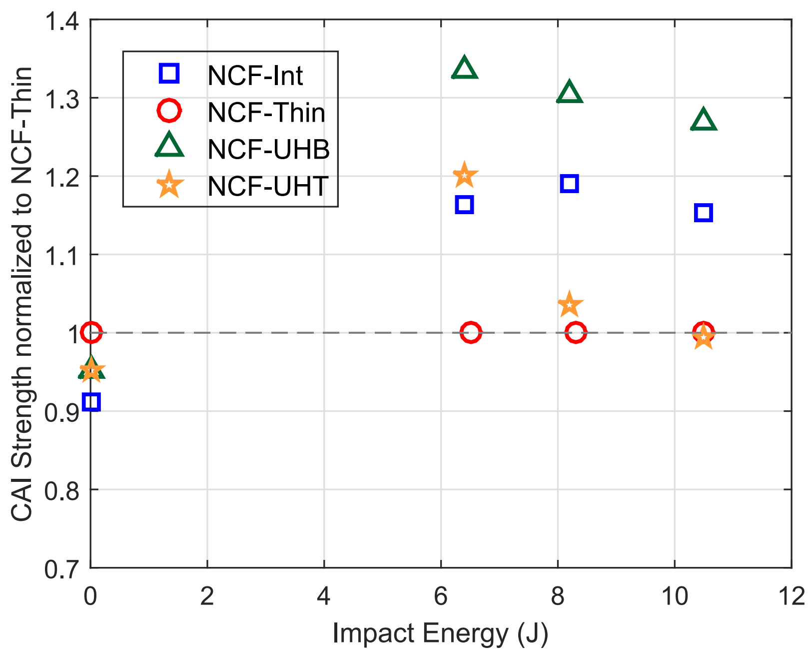

(b)

Figure 14: Comparison of CAI strengths normalised with (a) intermediate plies (NCF-Int) as baseline and (b) thin plies (NCF-Thin) as baseline. The plain compression strengths are also normalized according to the respective baselines.

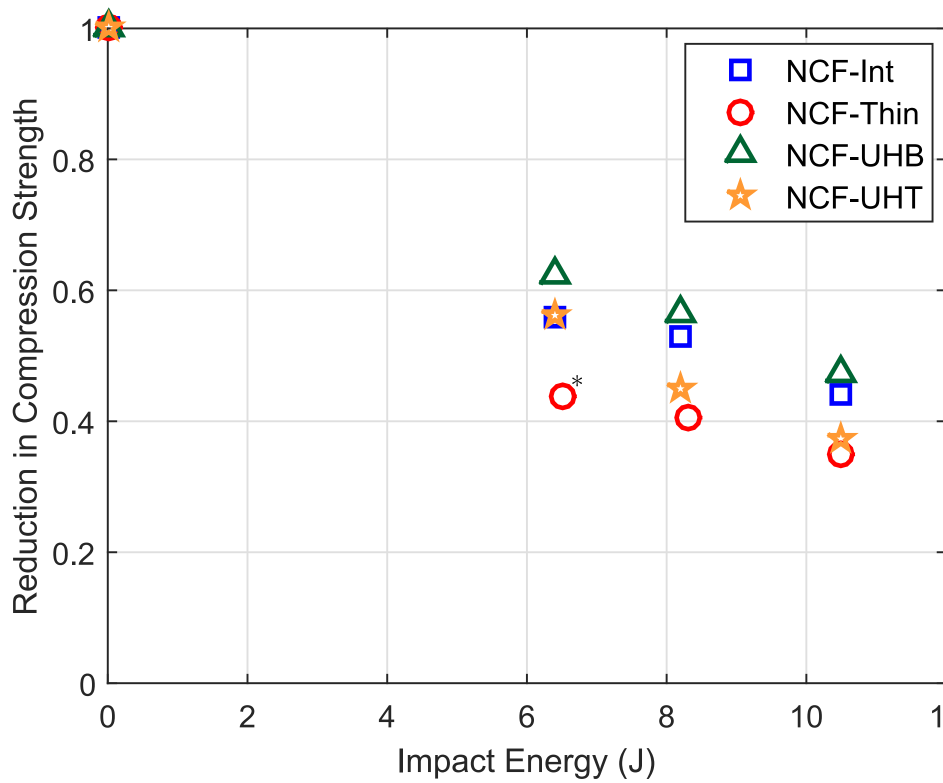

*CAI failure at the specimen top due to local buckling

Figure 15: Normalized reduction in the compressive strength due to the impact damage of all laminates.

Table 1: Laminates and their details

Laminate	Description	Stacking sequence	Ply thickness (mm)	Laminate thickness (mm)	D* (Nm)
NCF-Int	Intermediate plies	$[(45/0)/(-45/90)/(22.5/-22.5)]_S$	0.134	1.61	18.6
NCF-Thin	Thin plies	$[(45/0)/(-45/90)/(45/0)/(-45/90)/(45/0)/(-45/0)]_S$	0.067	1.61	18.9
NCF-UHB	Hybrid (Int. and thin plies)	$[(90/-45)/(0/45)/(90/-45)/(0/45)/(90/-45)/(0/45)/(90/-45)/(0/45)/(45/0)_{268}/(-45/90)_{268}]$	0.134 & 0.067	1.61	18.8
NCF-UHT	Hybrid (Int. and thin plies)	$[(90/45)_{268}/(0/-45)_{268}/(-45/0)/(45/90)/(-45/0)/(45/90)/(-45/0)/(45/90)/(-45/0)/(45/90)]$	0.134 & 0.067	1.61	18.8